Original Article

Institution of MECHANICAL ENGINEERS

Journal of ENGINEERING IN MEDICINE

Proc IMechE Part H:
J Engineering in Medicine
1–12

DOI: 10.1177/09544119231193879
journals.sagepub.com/home/pih
Sage

Stress-strain and fatigue life numerical evaluation of two different dental implants considering isotropic and anisotropic human jaw

Marco De Stefano[1], Antonio Lanza[2], Ludovico Sbordone[3] and Alessandro Ruggiero[1]

Abstract

Dental prostheses are currently a valid solution for replacing potential missing tooth or edentulism clinical condition. Nevertheless, the oral cavity is a dynamic and complex system: occlusal loads, external agents, or other unpleasant events can impact on implants functionality and stability causing a future revision surgery. One of the failure origins is certainly the dynamic loading originated from daily oral activities like eating, chewing, and so on. The aim of this paper was to evaluate, by a numerical analysis based on Finite Elements Method (FEM), and to discuss in a comparative way, firstly, the stress-strain of two different adopted dental implants and, subsequently, their fatigue life according to common standard of calculations. For this investigation, the jawbone was modeled accounting for either isotropic or anisotropic behavior. It was composed of cortical and cancellous regions, considering it completely osseointegrated with the implants. The impact of implants' fixture design, loading conditions, and their effect on the mandible bone was finally investigated, on the basis of the achieved numerical results. Lastly, the life cycle of the investigated implants was estimated according to the well-established theories of Goodman, Soderberg, and Gerber by exploiting the outcomes obtained by the numerical simulations, providing interesting conclusions useful in the dental practice.

Keywords

Dental implants, human mandible, stress-strain, finite element method, fatigue, biotribology

Date received: 2 March 2023; accepted: 25 July 2023

Introduction

Since 1965 with Brånemark first experience,[1] dental implants have been adopted in more and more human oral cavities. The possibility of replacing missing teeth has currently reached a rate of success near the 90%[2] or, in some circumstances, even higher.[3,4] However, several risks connected with patients' clinical conditions and with the chosen surgical procedure,[5] could compromise the functionality of medical instruments, causing severe diseases to the patients.[6] In addition, the occlusal forces, arisen from oral daily activities like eating or involuntary actions such as the bruxism, may generate mechanical complications to the implants.[7] Indeed, the loading forces variable in modulus and direction, have a great influence on the prosthesis functionality, as much as on the osseointegration process, defined as the functional connection between living bone and implanted system.[8] Indeed, in terms of stress, they are more impacting[9] than the static ones (5%–10%) and therefore more dangerous not only for the implant life, but also for the surrounding bone integrity. Moreover, when the mechanical stresses are coupled with corrosion phenomena due to the oral acid environment, the synergy between them can worse the scenario, causing bone and prosthesis stability loss.[10] In that sense, the fatigue effects, seen as the repetition

[1]Department of Industrial Engineering, University of Salerno, Fisciano, Italy
[2]Department of Medicine, Surgery and Dentistry "Schola Medica Salernitana," University of Salerno, Baronissi, Italy
[3]Department of Medicine and Health Sciences, University of Molise, V Campobasso, Italy

Corresponding author:
Marco De Stefano, Department of Industrial Engineering, University of Salerno, Via Giovanni Paolo II, nr. 132, Fisciano 84084, Italy.
Email: mardestefano@unisa.it

of cyclic stress of value lower than a maximum tolerable strength, could weaken the material up to its probable fracture.[11,12] Unfortunately, there are no current monitoring methods[13] of the first microfractures, which represent almost the totality of the failure (90%).

Consequently, in order to avoid this undesired occurrence, several studies have been conducted in the last years, with the aim of investigating and analyzing the fatigue behavior of dental implants. Ziaie and Khalili,[14] by using a Finite Element Analysis (FEA), noted that the abutment may be a critical component of the total assembly. In addition, they found that the root of the implant body screw, in proximity of the bone level, had the greatest probability of failure. Obviously, the design, as much as its topography and surface state, are key variables of the implant's duration[15] as much as the biological state of the bone.[16] In fact, Pérez[17] considered the impact of the diameter, together with fatigue material properties and loading conditions, by means of a probabilistic method, stating that the upper screw thread had the highest probability to fail. Ayllón et al.,[18] instead, proposed a theoretical model, split in the two phases of initiation and propagation, comparing their results with experimental tests. Pérez et al.[19] evaluated the effect of the addiction of zirconium to the titanium alloy, observing an increase of fatigue limit, respect to the pure titanium grade 4. An alternative to titanium alloys, is the PEEK (poly-ether-ether-ketone) material which is able to resist to the efforts caused by canonical masticatory cycles as confirmed by Schwitalla et al.[20] Hamed et al.[21] examined several articles published in the last 20 years regarding the diameter impact on the efficiency of fatigue, finding out that narrow ones (3–3.4 mm) are more likely to fail. Sun et al.[22] analyzed, by FEA, the influence of screw taper angle, observing that the 30° case had less wear and anti-loosening performance but lower life cycle than 180° one. He also evaluated the impact of loading angles and implant lengths[23]: the longer designs (11 vs 9 mm) presented better fatigue response whereas when the load angle increased, the fatigue life showed an exponential drop. In addition, the kind of abutment connection is also relevant as demonstrated by On et al.[24] and by Gil et al.[25] The thread type was investigated by Geramizadeh et al.[26] discovering that the combination of microthreads in the upper area and V-shape in the rest of the body provided the best distribution of stress. Aragoneses et al.,[27] instead, discussed the effect of roughness and material kind, noting that the former, which is even correlated with osteointegration process,[28] played a positive role on fatigue behavior. Finally, Shemtov-Yona and Rittel[29] studied the effect of oral solutions, realizing that the saline one was critical for the life of the implants, due to its peculiar aggressiveness. In this scientific framework, this manuscript aims firstly to calculate and discuss implants' stress/strain, by adopting a FEA, and, subsequently, to evaluate numerically also the fatigue life of two implant types which own diverse design in terms of diameter/length, fixing mechanism, and thread type. The contact zones between abutment and fixture were the center of discussion accounting for two different dental implants and two different jawbone types. The analysis was performed also including the bone anisotropy effects, under three load conditions. After that, an estimation of implants life, according to the three main common fatigue theories discussed in literature as Goodman, Soderberg, and Gerber[30] was achieved. The novelty of this investigation is related both to the numerical fatigue life estimation in a real human mandible, respect the most common ones founded in literature[31] performed by considering only a section of jawbone and to the comparison between two different systems. Indeed, despite several geometrical variables like diameter or fixing mechanism are involved in the analysis, the simultaneous action of each factor is not largely discussed in contrast with the study of the single parameter that has already been analyzed in literature. Moreover, the work includes the presence of recent ultrashort implants, which are yet not widely investigated,[32] especially under dynamic loads. In conclusion, different potential critical zones are arisen from the combination of the geometrical features of the two implants.

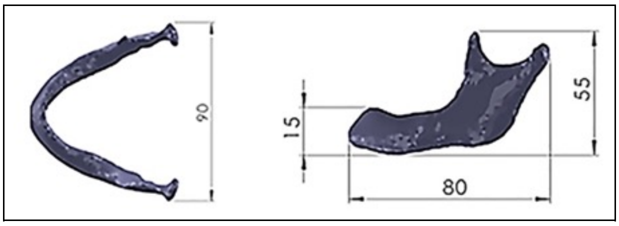

Figure 1. Human jaw dimensions (mm).

Materials and methods

The mandible considered in this work (Figure 1) was modeled by extrapolating a 3D scan file of a human jaw by Maco Guide software (produced by Media Lab, Piazza IV Novembre, 4, 20124 Milano, Italy) and successively imported in Autodesk MeshMixer 3.5 tool where it was cleaned and smoothed. Finally it was imported in SolidWorks 2020 where the mandible was coupled with the implants. The .STEP files generated, were imported in Ansys Workbench 2020 where the assembly was meshed in order to be processed by a stress/strain and fatigue analysis, in accordance with specific boundary conditions. The mandible was considered composed of both cortical and cancellous layer with variable thickness in the range 2–3.5 mm. It was coupled with two implant types (named as System 1 and System 2), both in Titanium Grade V (Ti6Al4V) (Figure 2), which guarantees good mechanical features, such as great strength and excellent biocompatibility properties.[33] As shown in Figure 2(a), System 1 presents an internal hexagonal connection with a screw as

Table 1. Systems 1–2 geometrical features (mm).

Implants	Head implant diameter	Implant length	Thread type	Thread pitch	Connection abutment-implant
System 1	3.5	8	V-shape	1.2	Fixing screw
System 2	4.6	5	Inclined plateau	0.63	Morse taper

fixing mechanism between abutment and implant, whereas the System 2 a Morse taper (Figure 2(b)). The different geometrical characteristics are reported in Table 1, but both have a cut zone for promoting osteointegration. In addition, as can be observed, the System 1 is a commonly used implant, whereas the second one is an ultrashort one (implant length < 6 mm) with greater diameter.[34] Besides the thread is different: V-shape of 1.2 mm pitch for the System 1 and inclined plateau of 0.63 mm pitch for the second. They were positioned in the canine zone and considered completely osseointegrated with the bone by a bonded coupling which provides no gap and does not permit any sliding, reinforced with Augmented Lagrange formulation[35] for avoiding potential penetrations. Moreover, as contact discretization, the algorithm node-to-segment was chosen in which the node of one surface is coupled with the segment of the other ones following the principle of closest point. The assembly did not involve natural teeth[17] but only the jawbone coupled with the implant,[36] since the crown material has not a significant effect on the assembly stress distribution.[37] This is confirmed also by Wieja et al.[38] regarding the bone deformations, strongly correlated with the mandible's geometry. The stress is mainly explicated in the implant-bone interface,[39] and the main causes of failure are related to potential inflammations or to the implant overload and its coupling with the bone,[7,40–43] which is the main focus of this investigation.

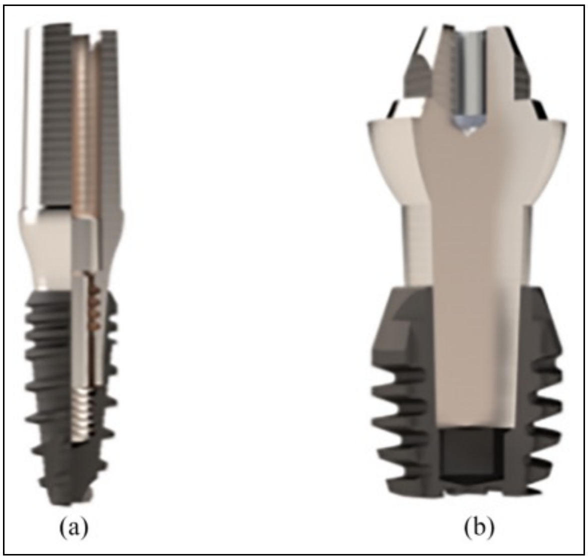

Figure 2. The two implants: (a) System 1 $\phi 3.5 \times 8$ mm and (b) System 2 $\phi 4.6 \times 5$ mm.

The mechanical properties such as Young's Modulus, Poisson's ratio, tensile yield, ultimate strength, and shear modulus of the bodies are shown in Table 2. The systems were considered as isotropic (equation (1)) and elastic, while for the bone even the anisotropic characteristics[44] were taken in account. In particular, the elastic regime for the cortical followed a transversely isotropic behavior (equation (2)), whereas the cancellous the orthotropic one (equation (3)).The mechanical relations are then coupled with the external forces. In particular, three types of load conditions were considered in this research. One simulates the average force of mastication explicated in the three directions[45]: 114.6 N in the vertical direction, 17.1 N in the lingual direction, and 23.4 N in the disto-mesial direction. The second and the third ones are of 200 N in modulus, which is even adopted in literature, being another common bite force value,[46] but the former is purely compressive, whereas the latter is oblique of 45° respect to the vertical axis in the buccal direction. They were all applied on the head of the abutment (Figure 3(a)).[47] Finally, the imposed boundary conditions provided fixed support[48] in the upper extremities of the mandible (Figure 3(b)) blocking all the translations and rotations in that zone, leaving the rest of the assembly free to move.

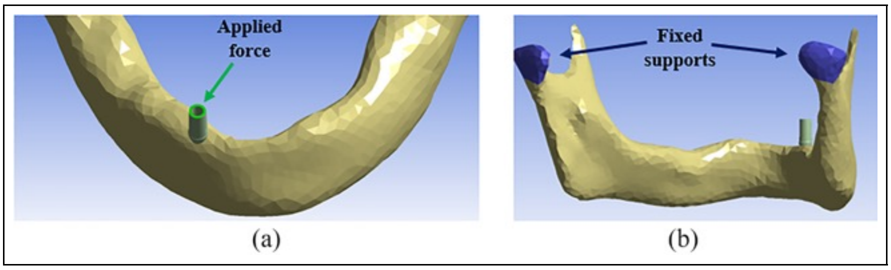

Figure 3. Boundary conditions of the coupling: (a) applied force and (b) fixed support.

$$\begin{pmatrix} \varepsilon_{xx} \\ \varepsilon_{yy} \\ \varepsilon_{zz} \\ \gamma_{xy} \\ \gamma_{xz} \\ \gamma_{yz} \end{pmatrix} = \begin{pmatrix} \frac{1}{E} & \frac{-\nu}{E} & \frac{-\nu}{E} & 0 & 0 & 0 \\ \frac{-\nu}{E} & \frac{1}{E} & \frac{-\nu}{E} & 0 & 0 & 0 \\ \frac{-\nu}{E} & \frac{-\nu}{E} & \frac{1}{E} & 0 & 0 & 0 \\ 0 & 0 & 0 & \frac{1}{G} = \frac{2(1+\nu)}{E} & 0 & 0 \\ 0 & 0 & 0 & 0 & \frac{1}{G} & 0 \\ 0 & 0 & 0 & 0 & 0 & \frac{1}{G} \end{pmatrix} \begin{pmatrix} \sigma_{xx} \\ \sigma_{yy} \\ \sigma_{zz} \\ \tau_{xy} \\ \tau_{xz} \\ \tau_{yz} \end{pmatrix} \quad (1)$$

$$\begin{pmatrix} \varepsilon_{xx} \\ \varepsilon_{yy} \\ \varepsilon_{zz} \\ \gamma_{xy} \\ \gamma_{xz} \\ \gamma_{yz} \end{pmatrix} = \begin{pmatrix} \frac{1}{E_x} & \frac{-\nu_{xy}}{E_x} & \frac{-\nu_{zx}}{E_z} & 0 & 0 & 0 \\ \frac{-\nu_{xy}}{E_x} & \frac{1}{E_x} & \frac{-\nu_{zy}}{E_z} & 0 & 0 & 0 \\ \frac{-\nu_{xz}}{E_x} & \frac{-\nu_{yz}}{E_x} & \frac{1}{E_z} & 0 & 0 & 0 \\ 0 & 0 & 0 & \frac{1}{G_{xy}} = \frac{2(1+\nu_{xy})}{E_x} & 0 & 0 \\ 0 & 0 & 0 & 0 & \frac{1}{G_{xz}} & 0 \\ 0 & 0 & 0 & 0 & 0 & \frac{1}{G_{yz}} \end{pmatrix} \begin{pmatrix} \sigma_{xx} \\ \sigma_{yy} \\ \sigma_{zz} \\ \tau_{xy} \\ \tau_{xz} \\ \tau_{yz} \end{pmatrix} \quad (2)$$

were chosen since the high modeling complexity of the surfaces analyzed.[50] The element size was differentiated in accordance with the geometrical characteristics of the bodies, between bone (0.7 mm) and implants (1 mm). Slow and smooth transitions are adopted with fine span angle center: the first improved the element quality while the second the curvature of elements. A ones-step refinement was applied in the contact zones since crucial for this investigation. After the convergence process, the system provided about 2 million of nodes and 1.5 million of elements. The quality was good as confirmed by average skewness value of 0.29 and element quality of 0.64. Finally, the nonlinear simulations were carried out in Ansys 2020 tool, involving the large deformations due to the potential transition from elastic to plastic regime. The criterion adopted to solve them was the Newton-Raphson algorithm, whereas the Von Mises criterion was assumed for stress/strain evaluation (equations (4) and (5)).

$$\sigma_v = \sqrt{\frac{(\sigma_{xx}-\sigma_{yy})^2 + (\sigma_{yy}-\sigma_{zz})^2 + (\sigma_{zz}-\sigma_{xx})^2 + 6(\tau_{xy}+\tau_{yz}+\tau_{zx})^2}{2}} \quad (4)$$

$$\varepsilon_v = \left(\frac{1}{1+\nu}\right)\sqrt{\frac{(\varepsilon_{xx}-\varepsilon_{yy})^2 + (\varepsilon_{yy}-\varepsilon_{zz})^2 + (\varepsilon_{zz}-\varepsilon_{xx})^2 + 6(\varepsilon_{xy}+\varepsilon_{yz}+\varepsilon_{zx})^2}{2}} \quad (5)$$

$$\begin{pmatrix} \varepsilon_{xx} \\ \varepsilon_{yy} \\ \varepsilon_{zz} \\ \gamma_{xy} \\ \gamma_{xz} \\ \gamma_{yz} \end{pmatrix} = \begin{pmatrix} \frac{1}{E_x} & \frac{-\nu_{xy}}{E_y} & \frac{-\nu_{zx}}{E_z} & 0 & 0 & 0 \\ \frac{-\nu_{xy}}{E_x} & \frac{1}{E_y} & \frac{-\nu_{zy}}{E_z} & 0 & 0 & 0 \\ \frac{-\nu_{xz}}{E_x} & \frac{-\nu_{yz}}{E_y} & \frac{1}{E_z} & 0 & 0 & 0 \\ 0 & 0 & 0 & \frac{1}{G_{xy}} & 0 & 0 \\ 0 & 0 & 0 & 0 & \frac{1}{G_{xz}} & 0 \\ 0 & 0 & 0 & 0 & 0 & \frac{1}{G_{yz}} \end{pmatrix} \begin{pmatrix} \sigma_{xx} \\ \sigma_{yy} \\ \sigma_{zz} \\ \tau_{xy} \\ \tau_{xz} \\ \tau_{yz} \end{pmatrix} \quad (3)$$

Concerning the mesh, instead, a combination of quadratic hexahedrons and tetrahedrons elements[49]

Lastly, the fatigue tests were conducted on the two systems in the same boundary conditions previously described, and they were evaluated in terms of life, safety factor, biaxiality indication, and fatigue sensitivity.[51] In particular, a fully reversed load was applied for each force step, and a value of 2000 cycles per day was assumed which corresponds an average value obtained by supposing two meals of 15 min at the rate of 1 Hz for a total of 1800. The lasting 200 were attributed to other mouth movements such as talking or bruxism. The basis hypothesis of the study were the S-N curves for Titanium Grade V, which were extrapolated from literature,[52] and the infinite life criteria sets equal to 10^{10} cycles. At the end, the safety factor (SF)

Table 2. Mechanical properties of the bodies.

Material	Body	Young's modulus E (GPa)	Poisson's ratio ν	Tensile yield strength σ_y (MPa)	Ultimate tensile strength σ_u (MPa)	Shear modulus G (GPa)
Titanium Grade V (Ti6Al4V)	Systems	110	0.32	830	900	/
Isotropic cortical	Cortical bone	13	0.30	102	118	/
Isotropic cancellous	Cancellous bone	1.3	0.30	21	25	/
Anisotropic cortical	Cortical bone	$E_x = 9.6$ $E_y = 9.6$ $E_z = 17.8$	$\nu_{xy} = 0.55$ $\nu_{yz} = 0.3$ $\nu_{xz} = 0.3$	115	133	$G_{xy} = 3.097$ $G_{yz} = 3.51$ $G_{xz} = 3.51$
Anisotropic cancellous	Cancellous bone	$E_x = 0.144$ $E_y = 0.099$ $E_z = 0.344$	$\nu_{xy} = 0.23$ $\nu_{yz} = 0.11$ $\nu_{xz} = 0.13$	32.4	37.5	$G_{xy} = 0.053$ $G_{yz} = 0.063$ $G_{xz} = 0.045$

Table 3. Maximum, minimum, and average stress values of System 1 in case of isotropic bone for the three load steps.

Loads (N)	Minimum (MPa)	Maximum (MPa)	Average (MPa)
Load 1 (17.1, 23.4, 114.6)	9.76×10^{-3}	680.15	15.02
Load 2 (200-vertical)	4.91×10^{-2}	1518.9	17.69
Load 3 (200-45°oblique)	1.75×10^{-2}	675.55	48.78

was extrapolated by the three theories of Goodman (equation (8)), Soderberg (equation (9)), and Gerber (equation (10)). The first two describe the relationship between the mean and the alternating stresses by a straight line with the difference that Soderberg adopts the yield and not the ultimate strength. On the contrary, Gerber assumes parabola approximation. By intersecting these curves with the stress applied, it is possible to calculate the SF value. To achieve that, since the three laws correlate the alternating and mean stresses, the first step was the calculation of alternating stress (σ_a) and mean stress (σ_m) as shown in (6) and (7):

$$\sigma_a = \frac{\sigma_{\max} - \sigma_{\min}}{2} \tag{6}$$

$$\sigma_m = \frac{\sigma_{\max} + \sigma_{\min}}{2} \tag{7}$$

Where $\sigma_{\max}$ and $\sigma_{\min}$ are the maximum and minimum Von Mises stress obtained from FEM analysis.

$$\left(\frac{\sigma_a}{\sigma_e}\right) + \left(\frac{\sigma_m}{\sigma_u}\right) = \frac{1}{SF} \qquad \textit{Goodman Theory} \tag{8}$$

$$\left(\frac{\sigma_a}{\sigma_e}\right) + \left(\frac{\sigma_m}{\sigma_y}\right) = \frac{1}{SF} \qquad \textit{Soderberg Theory} \tag{9}$$

$$\left(\frac{SF \cdot \sigma_m}{\sigma_u}\right)^2 + \left(\frac{SF \cdot \sigma_a}{\sigma_e}\right) = 1 \qquad \textit{Gerber Theory} \tag{10}$$

With σ_e endurance limit of 140 MPa,[52] σ_y and σ_u respectively yield strength and ultimate strength (Table 2).

Results and discussion

In this section the results obtained by FEM simulations will be analyzed and discussed according to the main literature outcomes of the recent years. Before dealing with the core of the work, the fatigue analysis, the static stress investigations of the implants and of the bone, taking in account its anisotropy and the implant type, are presented. In this way a comparison of the several effects of static and dynamic loads is achievable on diverse systems providing different critical zones emerged from the specific geometrical features of the implant.

Static stress/strain analysis

The two systems were subjected to three different load steps of diverse module and directions. In Table 3 are reported the maximum, minimum, and average stress values for the System 1 in case of isotropic bone. In this way the total range and average stress, extrapolated by FEM simulations and reported even in several similar investigations,[53–57] are given, since the peaks are not sufficient to describe the global mechanical behavior of the implants interesting just a restricted zone of the prosthesis. In this light, the average stress can approximate, thus, the total stress field of the medical tool, in a more precise and correct way than the minimum and maximum peaks. Moreover, the results are not strongly affected by potential numerical errors arisen from mesh features. To achieve that, the implant was firstly isolated from the jawbone and successively the average Von Mises stress was evaluated by summing up the stress on the volume of the single element and then dividing that sum by total volume. This index may be significantly helpful from a biological point of view since describing the mechanical response of the bone. Indeed, accordingly to Wolff's law, the latter remodels itself respect to the effort applied. Consequently, if the values are extremely great severe deformations can happen, but, on the other hand, if are too low bone resorption may occur[58] leading to bone density reduction and to prosthesis risk failures. As can be observed, the highest stress is referred to the pure compression, whereas the minimum for the Load 1. Interesting is the average stress value, which is approximately twice or three times when the load is oblique of 45° respect to the load along the vertical axis. Similar trends were observed also when the anisotropy is considered (Tables 4 and 5) but with an increase in the peaks. Hence, the effect of load inclination is relevant issue, as stated in literature,[32,59] providing greater average stress when the oblique force is applied.

For System 2, instead, as represented in Table 6, the Load 3 determined a rise in average stress of 60% and 45% respect to the Load 1 and 2, similarly to the previous system.

Comparing the implant types, Tables 3 and 6 confirm that the System 2 owns lower peak values of stress, far below the yield and the ultimate strength. On the other hand, the average and the minimum ones resulted higher. This can be explained by considering that the System 2 owns a higher diameter, but it is shorter than the System 1. Since both the geometrical variables are

Table 4. Maximum, minimum, and average stress values of System 1 in case of anisotropic bone for the three load steps.

Loads (N)	Minimum (MPa)	Maximum (MPa)	Average (MPa)
Load 1 (17.1, 23.4, 114.6)	2.49×10^{-2}	848.1	15.29
Load 2 (200-vertical)	2.81×10^{-2}	2072.4	19.10
Load 3 (200-45°oblique)	5.21×10^{-2}	963.12	47.58

Table 5. Maximum, minimum, and average stress values of System 2 in case of anisotropic bone for the three load steps.

Loads (N)	Minimum (MPa)	Maximum (MPa)	Average (MPa)
Load 1 (17.1, 23.4, 114.6)	0.14	212.65	19.98
Load 2 (200-vertical)	0.38	611.45	28.98
Load 3 (200-45°oblique)	0.47	264.93	46.83

Table 6. Maximum, minimum, and average stress values of System 2 in case of isotropic bone for the three load steps.

Loads (N)	Minimum (MPa)	Maximum (MPa)	Average (MPa)
Load 1 (17.1, 23.4, 114.6)	0.39	149.12	17.78
Load 2 (200-vertical)	0.92	386.46	24.99
Load 3 (200-45°oblique)	0.78	258.66	45.06

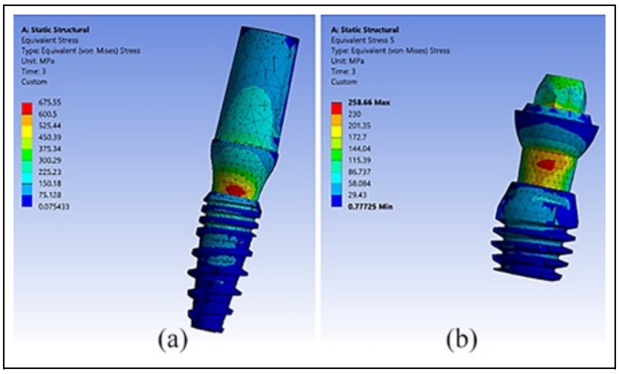

Figure 4. Stress map of (a) System 1 and (b) System 2 under Load 3 in case of isotropic bone.

influential,[60] their synergy determine the pressure distribution of Figure 4. Regarding the position of the maximum, instead, the abutment and the neck of the implant, in both the configurations are the most critical zones[61] as underlined in the image below. Unsurprisingly, the interface abutment-implant and the kind of fixing mechanism are crucial areas and currently object of investigation, especially by clinical trials.[62]

Giving a look to the values, although the minimum and the average are almost similar to the previous results, the maximum are, instead, higher in both cases. Consequently, considering the bone isotropic in numerical simulations is a significant limitation. Moreover, the System 1, in contrast with the second one, owns a screw as fixing mechanism which, as stated in literature, could represent a future failure risk,[63] particularly in cyclic loading. As proof, the total deformation of that component, for the Load 1, is reported. The deformation range is, for this coupling condition, 1.67 mm for the head of the screw-1.77 mm for the last four threads, and essentially directed to the vertical axis (90% of the total), followed by lingual (7%) and disto-mesial (3%) ones. The micromovements between implant and abutment should be kept in consideration since they represent a form of instability potentially correlated with the gap formation[64] and bacteria diffusion (microleakage). In conclusion, the System 1 showed higher values of micromotions, for all the boundary conditions, than System 2, as a result of the typical presence of the screw.[65]

Regarding the bone behavior, Von Mises elastic strain was taken in account. As indicated by Piccinini et al.[66] the bone health can be investigated in reference to the microstrain $\mu\varepsilon$: when it is lower than 1000, bone atrophy can occur, whereas above 3000 bone damage and adsorption may happen, and mechanical fracture when $\mu\varepsilon$ is above 25,000. Hence, the *optimal* range should be 1000–3000 $\mu\varepsilon$, which cannot be guaranteed in all the zones of the interface bone-implant since many variables, both clinical and mechanical variables like load, bone properties, materials adopted, are involved.[67] For instance, the former impacts on the strain regime determining a good range for Load 1 as shown in Figure 5 but not for the others two (Figure 6) with values near the fracture limit.

On the other hand, concerning the anisotropic behavior of the jaw, as stated in literature, it has a significant effect on efforts diffusion in bone-implant interface.[68,69] Indeed, a relevant drop on the peak strain values was

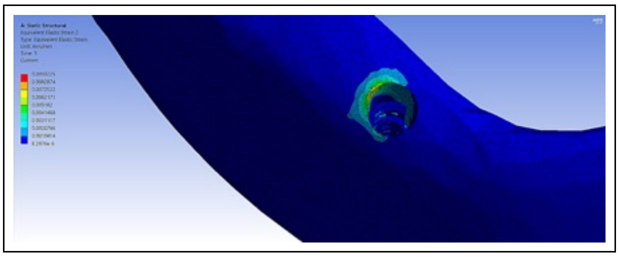

Figure 5. Isotropic mandible bone strain coupled with System 1 under Load 1.

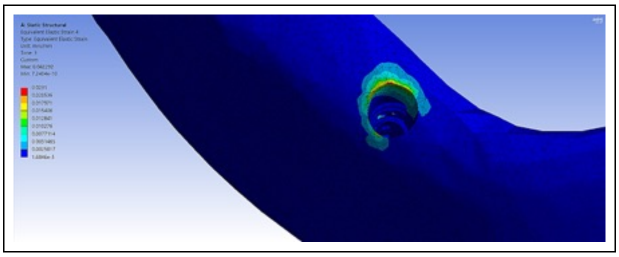

Figure 6. Isotropic mandible bone strain coupled with System 1 under Load 3.

noted when the bone behavior had been changed from anisotropic to isotropic of about 41% and 8% respectively for Systems 1 and 2. Similar trends were observed for the average strained area. This has a direct consequence on implant mechanical behavior and on micro-sliding with the bone. Hence, the bone properties plays a key role in the stress distribution and implant stability.[70] Finally, as well as the strain range, also the stress should be investigated because the yield strength, which determines the transition from elastic to plastic regime (102 or 115 MPa for cortical bone and 21 or 32 MPa for cancellous bone), can be passed over, circumstance that should be avoided since inducing permanent deformation in the bone. This happens in restricted zones located at cortical crest level under the Load 3 for both systems and bone configurations. Moreover, the maximum is located in cortical layer and not in the cancellous, being less rigid[71] as indicated by Young's modulus (Table 2). In particular, the cancellous stress is about 4%–10% of cortical layer, for all the cases analyzed.

In the next section these variables will be discussed under cyclic dynamic loads which could represents one of the most important implant failure cases.

Fatigue analysis

The fatigue test were performed according to a completely reversed loading simulating alternating tensile and compressive stress. The choice depends on the great variability of biting forces adopted in literature,[15] both in direction and modulus. In this way, several cases, even representing the worst scenario, are covered. First of all, many causes have been considered as triggering ones the implant fracture, like the developed loads, prosthesis design and position, and bone resorption.[72] Starting from the life of the System 1, it had the minimum, for all forces and bone configurations, in the fixing screw. The object has infinite life in all the zones with the exception of limited spots where it is subjected to failure. Although they are restricted area, they result very dangerous because they may spread out toxic titanium ions in the neighbor tissues, causing inflammations[73] or severe biological reactions such as cell necrosis.[74] Actually the fixing screw (Figure 7(a)) was not the only critical structure, but also the abutment-implant interface,[14] when the Load 3 is applied, as underlined just below (Figure 7(b)). This happens even when the anisotropy effect is adopted, reducing the lifetime from about 360 cycles to 127 cycles.

Besides, it is important to assess the impact of dynamic loads, respect to the static ones, which are certainly more realistic and closer to oral cavity biomechanical behavior. As stated in literature the safety factor has various calculations methods but all with the same meaning: how much stress can the structure withstand before it fails. If in static structural analysis is meant as

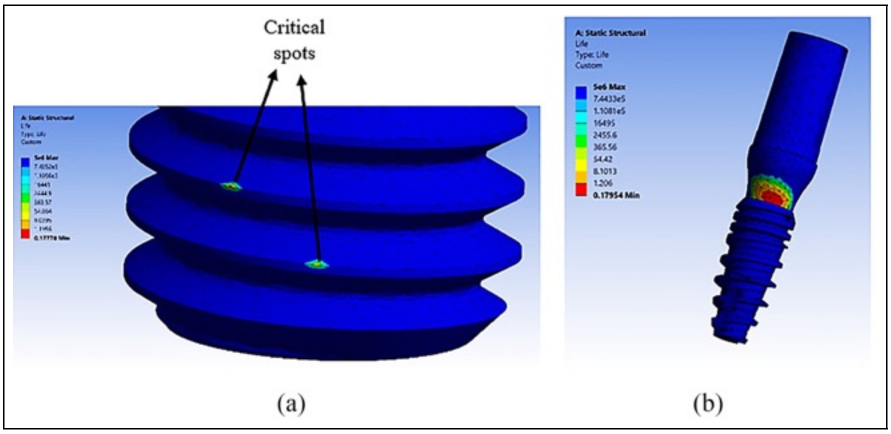

Figure 7. System 1 life under the Load 3 in case of isotropic bone: (a) fixing screw with critical spots and (b) implant coupled with the abutment.

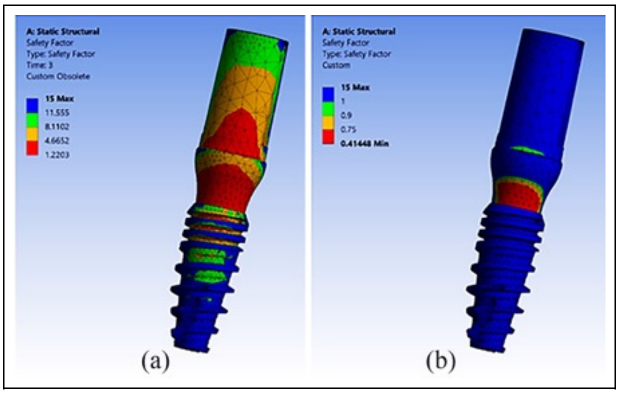

Figure 8. SF map of System 1 under Load 1: (a) static and (b) dynamic load.

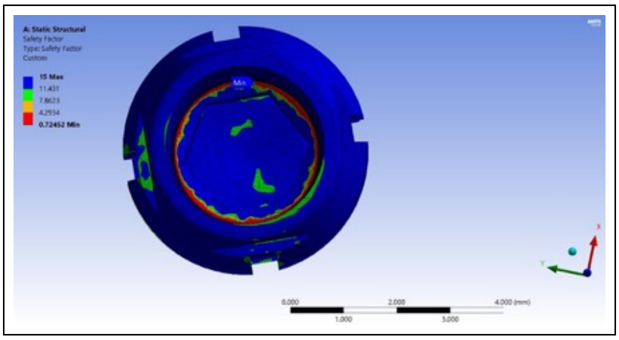

Figure 9. Safety factor of System 2 under the Load 2 and in case of isotropic bone.

the ratio between ultimate (or yield) strength and effective stress, in fatigue tool is the factor of safety with respect to a fatigue failure at a given design life. However, in both circumstances when it is lower than 1, the system cannot tolerate the imposed loads. Figure 8 highlights the two different kinds of load. It is possible to observe that not only the SF values are reduced but also the critical area of the entire structure became higher (interface implant-abutment). Hence, even if the implant was safe under static load, may fail under dynamic one.[75]

Focusing on the System 2, at first glance, seems to do not manifest the issues of Figure 7 thanks to its design and fixing mechanism. Indeed, as stated in literature, the geometrical features of an implant strictly influence the fatigue life. The second design, despite it is shorter, has a wider diameter than the other one that results in a lower probability to fail,[76] provides the Morse taper connection which has a better mechanical response respect to the internal hexagonal connection[77] and owns the inclined plateau thread which guarantees more contact area with the bone and thus less distributed stress.[78] Overall, the short design, with these geometrical features, could be considered as practical alternatives to common long ones for the treatment of atrophic jaws.[79]

Nevertheless, investigating more deeply the coupling and precisely the safety factor, a probable rupture zone is again in the interface implant-abutment (Min in the Figure 9) when the Load 2 is applied.

Lastly, considering that the life cycle of implants is crucial for dental field, the safety factors were calculated by the three theories described before. Since there is not a universal criterion to decide which theory should be adopted,[80] in the next graph the SF figures were calculated, for all coupling conditions, with Gerber theory. In Tables 7 to 10 the obtained results are showed, relating to the other two considered theories. By tracing a black line in correspondence to the upper limit of SF (Figure 10), it is almost clear that the System 2 performs better than the System 1 in all the configurations. Moreover, the lowest value are referred

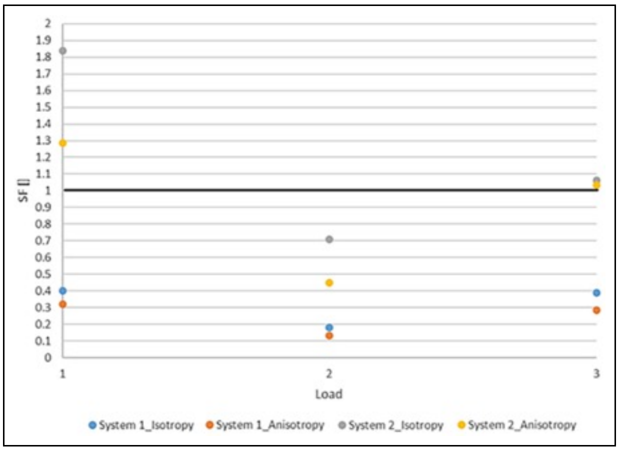

Figure 10. SF values of all coupling conditions according to Gerber's theory.

to the Load 2 step, thus when the stress is essentially composed of pure tensile and compression with no inclination. In addition, the anisotropy effect is visible in the reduction of SF in all the instances. Finally, a fatigue sensitivity investigation was carried out in order to understand the available life also in the cases of SF > 1: it was found that the System 2 presents no level of criticality under the Load 1 but a limit of about 3×10^6 cycles (about 1500 days) when the Load 1 is incremented of 50%.

In conclusion, the biaxiality indication was used with aim of figuring out the kind of stress state. Since the latter is included in the interval $[-1, 1]$ with -1 pure shear, 0 uniaxial stress, and $+1$ pure biaxial state, the simulations provided a marked variability of the results with the prevalence of biaxial stress for abutment and pure shear for the implant. By matching the SF and biaxiality indication, as expected, most damaged areas were under the pure shear.

Conclusions

This manuscript investigated the static and dynamic fatigue of two different dental implants, also involving the anisotropy of the bone, by using non-linear FEM

Table 7. Safety factor (SF) for System 1 and isotropic bone according to the three theories of Goodman, Gerber, and Soderberg.

Loads (N)	Goodman	Gerber	Soderberg
Load 1 (17.1, 23.4, 114.6)	0.356	0.402	0.352
Load 2 (200-vertical)	0.160	0.180	0.158
Load 3 (200-45°oblique)	0.359	0.389	0.355

Table 8. Safety factor (SF) for System 1 and anisotropic bone according to the three theories of Goodman, Gerber, and Soderberg.

Loads (N)	Goodman	Gerber	Soderberg
Load 1 (17.1, 23.4, 114.6)	0.286	0.323	0.283
Load 2 (200-vertical)	0.117	0.132	0.116
Load 3 (200-45°oblique)	0.252	0.284	0.249

Table 9. Safety factor (SF) for System 2 and isotropic bone according to the three theories of Goodman, Gerber, and Soderberg.

Loads (N)	Goodman	Gerber	Soderberg
Load 1 (17.1, 23.4, 114.6)	1.628	1.839	1.61
Load 2 (200-vertical)	0.628	0.709	0.542
Load 3 (200-45°oblique)	0.939	1.06	0.928

Table 10. Safety factor (SF) for System 2 and anisotropic bone according to the three theories of Goodman, Gerber, and Soderberg.

Loads (N)	Goodman	Gerber	Soderberg
Load 1 (17.1, 23.4, 114.6)	1.140	1.287	1.127
Load 2 (200-vertical)	0.397	0.448	0.392
Load 3 (200-45°oblique)	0.916	1.034	0.906

simulations[81] which is a common tool adopted in dentistry for exanimating the forces distribution.[82]

In the limitations of the considered assumptions, usually accepted in the scientific community, such as the complete osteointegration of the implants, the simplified loading scheme, the obtained results appear interesting and are summarized as follows:

1. the System 2 presents the best mechanical performance respect to System 1, both in static and dynamic results, thanks to its design and fixing mechanism. Although the former is shorter, the greater diameter as much as the absence of fixing screw, which is a critical component for System 1, permit a more favorable distribution of stress;
2. the anisotropy of the mandible's bone, which is an intrinsic property, has a significant impact on stress-strain regime inducing more efforts in the coupling and lower minimum SF values (from 0.158 to 0.116 for System 1 and from 0.542 to 0.392 for System 2). Hence, the isotropic behavior of jawbone is a clear limitation;
3. the compressive load (Load 2) showed the lowest SF for both implants and bone configurations;
4. the differences between static and dynamic loading were relevant: in some cases the implants showed a safe behavior under static conditions while not under the dynamic ones;
5. the critical rupture areas are localized in the proximity of the fixing screw for System 1, but also in the interface implant-abutment for specific boundary conditions;
6. most damaged areas in the implants were the zones subjected to pure shear.

We believe that even if the idea behind the presented investigation represents a contribute to the scientific knowledge and acts as basis for future developments, other investigations are required to achieve more and more data, especially by experimental and clinical investigations, including other load conditions, different bone mechanical properties, and more detailed oral environment.

Acknowledgement

We want to thank MaCo International, Industrial area-Buccino-Italy, for contributing to the research, providing us CAD models of implants.

Author contributions

Conceptualization: M. De Stefano and A. Ruggiero; Literature review: M. De Stefano, A. Lanza, L. Sbordone; Numerical calculations: M. De Stefano; Writing original draft preparation: M. De Stefano; Writing review and editing: M. De Stefano, A. Lanza, A. Ruggiero, L. Sbordone; Ethical Committee approval request: L. Sbordone; Theoretical supervision and methodology: A. Ruggiero.

Declaration of conflicting interests

The author(s) declared no potential conflicts of interest with respect to the research, authorship, and/or publication of this article.

Funding

The author(s) received no financial support for the research, authorship, and/or publication of this article.

Ethics approval and consent to participate

Comitato Bioetico Università degli Studi del Molise prot. n. 13700-II/23 del 29-03-2022.

ORCID iDs

Marco De Stefano https://orcid.org/0000-0001-5850-0014
Alessandro Ruggiero https://orcid.org/0000-0002-5111-2331

References

1. Abraham CM. A brief historical perspective on dental implants, their surface coatings and treatments. *Open Dent J* 2014; 8: 50–55.
2. Oh S-L, Shiau HJ and Reynolds MA. Survival of dental implants at sites after implant failure: a systematic review. *J Prosthet Dent* 2020; 123(1): 54–60.
3. Mangano C, Mangano F, Shibli JA, et al. Prospective evaluation of 2,549 Morse taper connection implants: 1- to 6-year data. *J Periodontol* 2011; 82(1): 52–61.
4. Karoussis IK, Brägger U, Salvi GE, et al. Effect of implant design on survival and success rates of titanium oral implants: a 10-year prospective cohort study of the ITI® Dental Implant System. *Clin Oral Implants Res* 2004; 15(1): 8–17.
5. Cakarer S, Selvi F, Can T, et al. Investigation of the risk factors associated with the survival rate of dental implants. *Implant Dent* 2014; 23(3): 328–333.
6. Becker ST, Beck-Broichsitter BE, Rossmann CM, et al. Long-term survival of Straumann dental implants with TPS surfaces: a retrospective study with a follow-up of 12 to 23 years. *Clin Implant Dent Relat Res* 2016; 18(3): 480–488.
7. Schwarz MS. Mechanical complications of dental implants. *Clin Oral Implants Res* 2000; 11 Suppl 1: 156–158.
8. Parithimarkalaignan S and Padmanabhan TV. Osseointegration: an update. *J Indian Prosthodont Soc* 2013; 13: 2–6.
9. Geramizadeh M, Katoozian H, Amid R, et al. Finite element analysis of dental implants with and without microthreads under static and dynamic loading. *J Long Term Eff Med Implants* 2017; 27(1): 25–35.
10. Sridhar S, Abidi Z, Wilson TG Jr, et al. In vitro evaluation of the effects of multiple oral factors on dental implants surfaces. *J Oral Implantol* 2016; 42(3): 248–257.
11. Velho HC, Dapieve KS, Valandro LF, et al. Cyclic fatigue tests on non-anatomic specimens of dental ceramic materials: a scoping review. *J Mech Behav Biomed Mater* 2022; 126: 104985.
12. Gherde C, Dhatrak P, Nimbalkar S, et al. A comprehensive review of factors affecting fatigue life of dental implants. *Mater Today Proc* 2021; 43(7): 1117–1123.
13. Shemtov-Yona K and Rittel D. An overview of the mechanical integrity of dental implants. *Biomed Res Int* 2015; 2015: 547384.
14. Ziaie B and Khalili SMR. Evaluation of fatigue life for dental implants using FEM analysis. *Prosthesis* 2021; 3: 300–313.
15. Shemtov-Yona K and Rittel D. Fatigue of dental implants: facts and fallacies. *Dent J* 2016; 4(2): 16.
16. Satpathy M, Duan Y, Betts L, et al. Effect of bone remodeling on dental implant fatigue limit predicted using 3D finite element analysis. *J Dent Oral Epidemiol* 2022; 2(1): 10.
17. Pérez MA. Life prediction of different commercial dental implants as influence by uncertainties in their fatigue material properties and loading conditions. *Comput Methods Programs Biomed* 2012; 108(3): 1277–1286.
18. Ayllón JM, Navarro C, Vázquez J, et al. Fatigue life estimation in dental implants. *Eng Fract Mech* 2014; 123: 34–43.
19. Pérez RA, Gargallo J, Altuna P, et al. Fatigue of narrow dental implants: influence of the hardening method. *Materials (Basel)* 2020; 13: 1429.
20. Schwitalla AD, Zimmermann T, Spintig T, et al. Fatigue limits of different PEEK materials for dental implants. *J Mech Behav Biomed Mater* 2017; 69: 163–168.
21. Hamed MT, Mously HA, Ghulman MM, et al. Impact of dental implant diameter on the efficiency of fatigue: a systematic review analysis. *J Pak Med Assoc* 2021; 71(6): 1648–1654.
22. Sun F, Lv LT, Xiang DD, et al. Effect of central screw taper angles on the loosening performance and fatigue characteristics of dental implants. *J Mech Behav Biomed Mater* 2022; 129: 105136.
23. Sun F, Lv LT, Cheng W, et al. Effect of loading angles and implant lengths on the static and fatigue fractures of dental implants. *Materials (Basel)* 2021; 14(19): 5542.
24. On SW, Yi SM, Park IY, et al. Fracture and fatigue of dental implants fixtures and abutments with a novel internal connection design: an in vitro pilot study comparing three different dental implant systems. *J Funct Biomater* 2022; 13(4): 239.
25. Gil FJ, Herrero-Climent M, Lázaro P, et al. Implant-abutment connections: influence of the design on the microgap and their fatigue and fracture behavior of dental implants. *J Mater Sci Mater Med* 2014; 25(7): 1825–1830.
26. Geramizadeh M, Katoozian H, Amid R, et al. Static, dynamic, and fatigue finite element analysis of dental implants with different thread designs. *J Long Term Eff Med Implants* 2016; 26(4): 347–355.

27. Aragoneses J, Valverde NL, Fernandez-Dominguez M, et al. Relevant aspects of titanium and zirconia dental implants for their fatigue and osseointegration behaviors. *Materials (Basel)* 2022; 15(11): 4036.
28. De Stefano M, Aliberti SM and Ruggiero A. (Bio)Tribocorrosion in dental implants: principles and techniques of investigation. *Appl Sci* 2022; 12: 7421.
29. Shemtov-Yona K and Rittel D. Fatigue failure of dental implants in simulated intraoral media. *J Mech Behav Biomed Mater* 2016; 62: 636–644.
30. Prados-Privado M, Prados-Frutos JC, Manchón Á, et al. Dental implants fatigue as a possible failure of implantologic treatment: the importance of randomness in fatigue behaviour. *Biomed Res Int* 2015; 2015: 825402.
31. Duan Y, Gonzalez JA, Kulkarni PA, et al. Fatigue lifetime prediction of a reduced-diameter dental implant system: numerical and experimental study. *Dent Mater* 2018; 34(9): 1299–1309.
32. Lee H, Park S and Noh G. Biomechanical analysis of 4 types of short dental implants in a resorbed mandible. *J Prosthet Dent* 2019; 121(4): 659–670.
33. Janeček M, Nový F, Harcuba P, et al. The very high cycle fatigue behaviour of Ti-6Al-4V alloy. *Acta Phys Pol A* 2015; 128(4): 497–503.
34. De Stefano M, Lanza A, Faia E, et al. A novel ultrashort dental implant design for the reduction of the bone stress/strain: a comparative numerical investigation. *Adv Biomed Eng* 2023; 5: 100077.
35. De Stefano M and Ruggiero A. Real contact area and friction. In: Katiyar JK, Ruggiero A, Rao TVVLN, et al. (eds) *Industrial tribology*. Boca Raton, FL: CRC Press, 2022, pp.1–23.
36. Flanagan D, Ilies H, McCullough P, et al. Measurement of the fatigue life of mini dental implants: a pilot study. *J Oral Implantol* 2008; 34(1): 7–11.
37. Wazeh AM, El-Anwar MI, Galal Atia RM, et al. 3D FEA study on implant threading role on selection of implant and crown materials. *Open Access Maced J Med Sci* 2018; 6(9): 1702–1706.
38. Wieja F, Jacobs G, Stein S, et al. Development and validation of a parametric human mandible model to determine internal stresses for the future design optimization of maxillofacial implants. *J Mech Behav Biomed Mater* 2022; 125: 104893.
39. Ghadiri M, Shafiei N, Salekdeh SH, et al. Investigation of the dental implant geometry effect on stress distribution at dental implant–bone interface. *J Braz Soc Mech Sci Eng* 2016; 38: 335–343.
40. Sakka S, Baroudi K and Nassani MZ. Factors associated with early and late failure of dental implants. *J Investig Clin Dent* 2012; 3(4): 258–261.
41. Gupta S, Gupta H and Tandan A. Technical complications of implant-causes and management: a comprehensive review. *Natl J Maxillofac Surg* 2015; 6(1): 3–8.
42. Han H-J, Kim S and Han DH. Multifactorial evaluation of implant failure: a 19-year retrospective study. *Int J Oral Maxillofac Implants* 2014; 29(2): 303–310.
43. Winkler S, Ring K, Ring JD, et al. Implant screw mechanics and the settling effect: an overview. *J Oral Implantol* 2003; 29(5): 242–245.
44. Cicciù M, Cervino G, Bramanti E, et al. FEM analysis of mandibular prosthetic overdenture supported by dental implants: evaluation of different retention methods. *Comput Math Methods Med* 2015; 2015: 943839.
45. Carter DR, Van Der Meulen MC and Beaupré GS. Mechanical factors in bone growth and development. *Bone* 1996; 18(1 Suppl): 5S–10S.
46. Winter W, Klein D and Karl M. Micromotion of dental implants: basic mechanical considerations. *J Med Eng* 2013; 2013: 265412.
47. Armentia M, Abasolo M, Coria I, et al. Fatigue design of dental implant assemblies: a nominal stress approach. *Metals* 2020; 10: 744.
48. Zhong S, Shi Q, Sun Y, et al. Biomechanical comparison of locking and non-locking patient-specific mandibular reconstruction plate using finite element analysis. *J Mech Behav Biomed Mater* 2021; 124: 104849.
49. Nihara J, Gielo-Perczak K, Cardinal L, et al. Finite element analysis of mandibular molar protraction mechanics using miniscrews. *Eur J Orthod* 2015; 37(1): 95–100.
50. Ruggiero A, D'Amato R and Affatato S. Comparison of meshing strategies in THR finite element modelling. *Materials (Basel)* 2019; 12(14): 2332.
51. Vidhya MS and Christina KVM. Fatigue life, fatigue damage, fatigue factor of safety, fatigue sensitivity, biaxiality indication and equivalent stress of a radial connecting rod. *Int J Res Eng Technol* 2020; 7(9): 1499–1502.
52. Kayabaşı O, Yüzbasıoğlu E and Erzincanlı F. Static, dynamic and fatigue behaviors of dental implant using finite element method. *Adv Eng Softw* 2006; 37: 649–658.
53. Valera-Jiménez JF, Burgueño-Barris G, Gómez-González S, et al. Finite element analysis of narrow dental implants. *Dent Mater* 2020; 36(7): 927–935.
54. Vidya Bhat S, Premkumar P and Kamalakanth Shenoy K. Stress distribution around single short dental implants: a finite element study. *J Indian Prosthodont Soc* 2014; 14(Suppl 1): 161–167.
55. Meriç G, Erkmen E, Kurt A, et al. Biomechanical comparison of two different collar structured implants supporting 3-unit fixed partial denture: a 3-D FEM study. *Acta Odontol Scand* 2012; 70(1): 61–71.
56. Canullo L, Pace F, Coelho P, et al. The influence of platform switching on the biomechanical aspects of the implant-abutment system. A three dimensional finite element study. *Med Oral Patol Oral Cir Bucal* 2011; 16(6): e852–e856.
57. Chang CL, Chen CS, Yeung TC, et al. Biomechanical effect of a zirconia dental implant-crown system: a three-dimensional finite element analysis. *Int J Oral Maxillofac Implants* 2012; 27(4): e49–e57.
58. Kitamura E, Stegaroiu R, Nomura S, et al. Biomechanical aspects of marginal bone resorption around osseointegrated implants: considerations based on a three-dimensional finite element analysis. *Clin Oral Implants Res* 2004; 15(4): 401–412.
59. Chun H-J, Cheong S-Y, Han J-H, et al. Evaluation of design parameters of osseointegrated dental implants using finite element analysis. *J Oral Rehabil* 2002; 29(6): 565–574.
60. Li T, Kong L, Wang Y, et al. Selection of optimal dental implant diameter and length in type IV bone: a three-dimensional finite element analysis. *Int J Oral Maxillofac Surg* 2009; 38(10): 1077–1183.
61. Maminskas J, Puisys A, Kuoppala R, et al. The prosthetic influence and biomechanics on peri-implant strain: a systematic literature review of finite element studies. *J Oral Maxillofac Res* 2016; 7(3): 4.

62. Rack A, Rack T, Stiller M, et al. In vitro synchrotron-based radiography of micro-gap formation at the implant–abutment interface of two-piece dental implants. *J Synchrotron Radiat* 2010; 17(Pt 2): 289–294.
63. Bicudo P, Reis J, Deus AM, et al. Performance evaluation of dental implants: an experimental and numerical simulation study. *Theor Appl Fract Mech* 2016; 85: 74–83.
64. Grobecker-Karl T and Karl M. Correlation between micromotion and gap formation at the implant-abutment interface. *Int J Prosthodont* 2017; 30(2): 150–152.
65. Larrucea Verdugo C, Jaramillo Núñez G, Acevedo Avila A, et al. Microleakage of the prosthetic abutment/implant interface with internal and external connection: in vitro study. *Clin Oral Implants Res* 2014; 25(9): 1078–1083.
66. Piccinini M, Cugnoni J, Botsis J, et al. Numerical prediction of peri-implant bone adaptation: comparison of mechanical stimuli and sensitivity to modeling parameters. *Med Eng Phys* 2016; 38: 1348–1359.
67. Korabi R, Shemtov-Yona K, Dorogoy A, et al. The failure envelope concept applied to the bone-dental implant system. *Sci Rep* 2017; 7: 2051.
68. O'Mahony AM, Williams JL and Spencer P. Anisotropic elasticity of cortical and cancellous bone in the posterior mandible increases peri-implant stress and strain under oblique loading. *Clin Oral Implants Res* 2001; 12: 648–657.
69. Bonnet AS, Postaire M and Lipinski P. Biomechanical study of mandible bone supporting a four-implant retained bridge: finite element analysis of the influence of bone anisotropy and foodstuff position. *Med Eng Phys* 2009; 31(7): 806–815.
70. Javed F and Romanos GE. The role of primary stability for successful immediate loading of dental implants. A literature review. *J Dent* 2010; 38(8): 612–620.
71. Merdji A, Bachir Bouiadjra B, Achour T, et al. Stress analysis in dental prosthesis. *Comput Mater Sci* 2010; 49(1): 126–133.
72. Tagger Green N, Machtei EE, Horwitz J, et al. Fracture of dental implants: literature review and report of a case. *Implant Dent* 2002; 11(2): 137–143.
73. Kim KT, Eo MY, Nguyen TTH, et al. General review of titanium toxicity. *Int J Implant Dent* 2019; 5(1): 10.
74. Kheder W, Al Kawas S, Khalaf K, et al. Impact of tribocorrosion and titanium particles release on dental implant complications - a narrative review. *Jpn Dent Sci Rev* 2021; 57: 182–189.
75. Senalp AZ, Kayabasi O and Kurtaran H. Static, dynamic and fatigue behavior of newly designed stem shapes for hip prosthesis using finite element analysis. *Mater Des* 2007; 28(5): 1577–1583.
76. Shemtov-Yona K, Rittel D, Levin L, et al. Effect of dental implant diameter on fatigue performance. Part I: mechanical behavior. *Clin Implant Dent Relat Res* 2014; 16(2): 172–177.
77. Prados-Privado M, Gehrke S, Rojo R, et al. Probability of failure of internal hexagon and Morse taper implants with different bone levels: a mechanical test and probabilistic fatigue. *Int J Oral Maxillofac Implants* 2018; 33(6): 1266–1273.
78. Hsieh HM and Hsu ML. Comparison of peri-implant bone stress with different implant crest module designed by 3D finite element analysis. *J Prosthodont Implantol* 2018; 7(4): 32–39.
79. de Oliveira Melo JMF, Willmersdorf RB, de Siqueira, Lages A, et al. Evaluation of stress and fatigue on different implant lengths in the rehabilitation of atrophic mandibles with full-arch fixed prosthesis using finite element method. *Int J Oral Maxillofac Implants* 2022; 37(5): 971–981.
80. Ferreño D, Casado JA, Carrascal IA, et al. Experimental and finite element fatigue assessment of the spring clip of the SKL-1 railway fastening system. *Eng Struct* 2019; 188: 553–563.
81. DeTolla DH, Andreana S, Patra A, et al. Role of the finite element model in dental implants. *J Oral Implantol* 2000; 26(2): 77–81.
82. Cortese A, Spirito F, Claudio PP, et al. Mandibular reconstruction after resection of ameloblastoma by custom-made CAD/CAM mandibular titanium prosthesis: two case reports, finite element analysis and discussion of the technique. *Dent J* 2023; 11(4): 106.